THE JOURNAL OF PHYSICAL CHEMISTRY A

pubs.acs.org/JPCA Article

Marcus Relationship Maintained During Ultrafast Electron Transfer Across a Supramolecular Capsular Wall

Aritra Das, Nareshbabu Kamatham, A. Mohan Raj, Pratik Sen,* and V. Ramamurthy*

Cite This: J. Phys. Chem. A 2020, 124, 5297−5305 Read Online

ACCESS | Metrics & More | Article Recommendations | Supporting Information

ABSTRACT: Photoinduced electron transfer across an organic capsular wall between excited donors and ground-state acceptors is established to occur with rate constants varying in the range 0.32−4.0 × 10^{11} s^{-1} in aqueous buffer solution. The donor is encapsulated within an anionic supramolecular capsular host, and the cationic acceptor remains closer to the donor separated by the organic frame through Coulombic attraction. Such an arrangement results in electron transfer proceeding without diffusion. Free energy of the reaction ($\Delta G°$) and the rate of electron transfer show Marcus relation with inversion. From the plot, λ and V_{el} were estimated to be 1.918 and 0.0058 eV, respectively. Given that the donor remains within the nonpolar solvent-free confined space, and there is not much change in the environment around the acceptor, the observed λ is believed to be because of "internal" reorganization rather than "solvent" reorganization. A similarity exists between the capsular assembly investigated here and glass and crystals at low temperature where the medium is rigid. The estimated electronic coupling (V_{el}) implies the existence of interaction between the donor and the acceptor through the capsular wall. Existence of such an interaction is also suggested by ^{1}H NMR spectra. Results of this study suggest that molecules present within a confined space could be activated from outside. This provides an opportunity to probe the reactivity and dynamics of radical ions within an organic capsule.

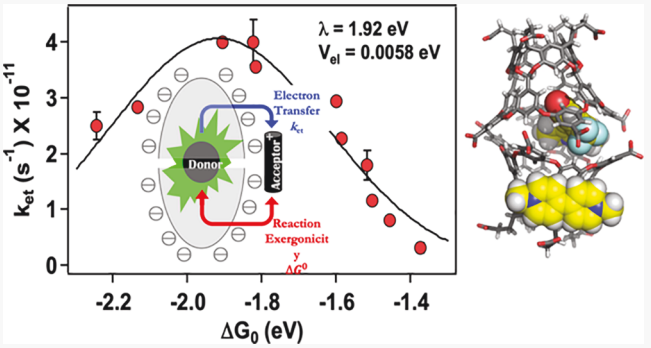

INTRODUCTION

Electron transfer plays a prominent role in several important events such as photosynthesis, solar energy storage, metabolic and respiratory processes, photocatalysis, electrical conduction in organic materials, and several organic and inorganic reactions.[1−6] In such studies, occurrence of electron transfer at short as well as long distances has been noted. The rate of electron transfer that occurs via the classic tunneling mechanism is established to exponentially increase with decrease in the donor−acceptor distance.[5] Challenging long-distance electron transfer investigations have involved protein,[7−12] DNA,[13−16] and hydrocarbon chains as scaffolds and covalently linked donor−acceptor systems.[17−20] In these systems, electron transfer occurs either through hopping or via superexchange mechanism involving σ or π bonds. In addition to these, there are systems wherein electron transfer occurs through noncovalent interactions,[17] in frozen and free solvents,[21−24] with the help of a solvent molecule trapped between a C-clamp molecule,[25−28] and in mixed donor−acceptor melts.[29−31] Interprotein electron transfer that involves solvent mediation belongs to this category.[10−12] These studies suggest that for electron transfer to occur, donor and acceptor molecules need not to be within collisional distance or covalently linked. The presence of another molecule in between a donor and an acceptor apparently would not inhibit the electron transfer, and its presence, in fact, is better than vacuum.[20]

Among supramolecular assemblies, to our knowledge, the Cram-type carcerand[32] is a unique assembly, where the donor and acceptor molecules could be well separated by the host wall. Energy and electron transfers have been established to occur between the donor and acceptor molecules, one trapped within the Cram-type carcerand and the other free outside in solution.[33−39] In fact, results reported with these systems have laid the groundwork for the current undertaking. Unfortunately, because the interior of the Cram-type carcerand is small, its generality is limited. Most guests need to be included during the synthesis of the carcerand.

In the current study, we employ a synthetic host known as octa acid (OA),[40] whose structure and internal dimensions are provided in Figure 1. Unlike Cram-type carcerand, the OA capsule is made up of two molecules of OA that assemble in

Received: May 3, 2020
Revised: June 3, 2020
Published: June 10, 2020

https://dx.doi.org/10.1021/acs.jpca.0c03944
J. Phys. Chem. A 2020, 124, 5297−5305

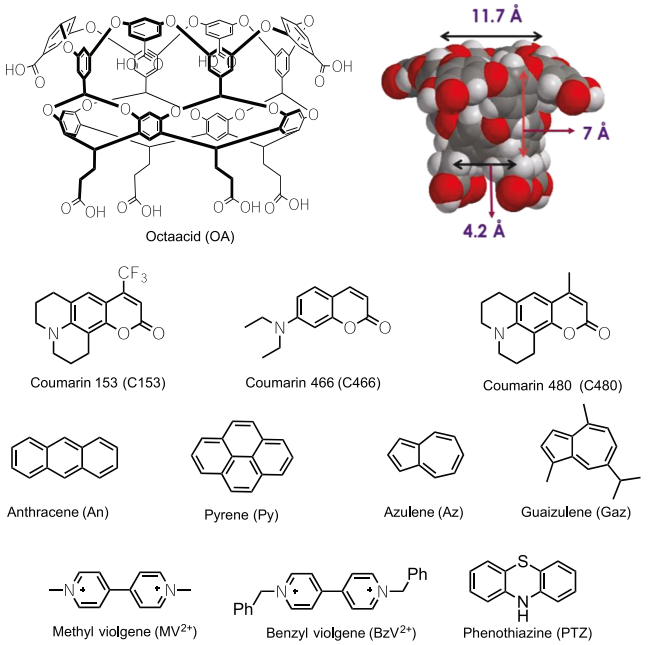

Figure 1. Chemical structure of donor and acceptor molecules used in the present study.

the presence of a hydrophobic guest molecule. This and larger internal dimension allow inclusion of a wider variety of guest molecules.[41] Importantly, the capsule is tight and takes a few milliseconds to partially open and close.[42,43] Therefore, during the time of electron transfer between the encapsulated excited donor and the acceptor, the capsule remains tightly closed similar to that of the Cram-type carcerand.[44]

Furthermore, prior studies have established the interior of the capsule to be dry and not to contain water molecules.[44,45] These would mean that prior to and after the electron transfer, only the interior wall of OA would surround the donor molecule. Because of the tightness of the capsule, at no stage during the excited-state lifetime of the donor there is a direct contact between the donor and acceptor molecules as well as between the donor and exterior water molecules. Therefore, the OA system, we have chosen, allows probing the importance of a permanent organic molecular wall during electron transfer between the encapsulated donor and free acceptor. One could visualize this to be a model for electron transfer across a solvent molecule that is permanently placed between the donor and the acceptor. Similarity between the current assembly and solvent-mediated C-clamp system,[27] the Cram-type carcerand assembly[35] and the solvent-separated radical ion pairs (SSRIPs)[46] are obvious. At the same time, the OA capsule-based system is unique: the wall is permanent, and the donor and acceptor are held closer by Coulombic attraction that makes the electronic coupling between the donor and acceptor stronger. We believe that the electronic coupling required for electron transfer between the encapsulated donor and nearby acceptor must involve the host wall.

We have recently demonstrated the occurrence of photo-induced electron transfer (PET) between OA-encapsulated donors [stilbene, coumarins, and azulenes (Az's)] and methyl viologen acceptor in phosphate/borate buffer solution (pH ~ 7.4 and 8.7).[47−52] Through time-resolved experiments, we have identified the formation of methyl viologen radical cation as well as stilbene radical cation, the products of electron transfer. With the help of ultrafast time-resolved experiments, the forward electron transfers were found to occur with time constants between 1 and 25 ps. Although the above experiments unequivocally established the occurrence of electron transfer across the capsular wall, the mechanism is not clear. Based on known lower β values of solvents such as tetrahydrofuran and water (1.2 and 1.68 $Å^{-1}$, respectively) with respect to vacuum (3.5 $Å^{-1}$),[22,23,53] we believe that the capsular wall can transport electron from the encapsulated excited donor to free acceptor and will not be passive. Similar to solvent molecules, one would expect the OA frame that is made up of electron-rich benzyl units to have lower β value, certainly well below vacuum. However, unlike solvent molecules, the OA frame is not soft and flexible.[54] Because of this, the OA cavity would not be expected to help prepare the excited donor for electron transfer (conversion of D to $D^{+\bullet}$), although it might help transport an electron across the wall. The current experiments are directed toward understanding: (a) whether the electron transfer occurs by the superexchange mechanism involving the host wall or via the classic tunneling by-passing the wall, (b) whether it proceeds via adiabatic or nonadiabatic pathway, that is, how strong is the electronic coupling (V_{el}) between the reactant and the product, and (c) what is the value of reorganization energy (λ) as defined by the Marcus equation.[55−58] We expected that study of a series of donor−acceptor pairs with varying $\Delta G°$ values would provide answers to the above questions. With this in mind, we have investigated electron transfer between donors and acceptors, as listed in Figure 1. In the following sections, results of these experiments are presented and discussed. Interestingly, the Marcus relationship between the rate and $\Delta G°$ was noted, and a nonzero value for V_{el} was calculated from the plot. Unexpectedly, a higher λ value (reorganization energy) was revealed, which is possibly a consequence of the rigidity surrounding the donor.

EXPERIMENTAL SECTION

Materials. Coumarin 153 (C153), coumarin 466 (C466), and coumarin 480 (C480) were purchased from Exciton Inc., high-purity pyrene (Py), anthracene (An), Az, and guaiazulene (Gaz) were purchased from Sigma-Aldrich, and methyl viologen dichloride dihydrate (MV^{2+}) and benzyl viologen dichloride (BzV^{2+}) purchased from Sigma-Aldrich and phenothiazine (PTZ) purchased from TCI Chemicals were used as received. OA was synthesized and purified by following the published procedure and characterized by NMR spectroscopy.[40] Spectroscopic-grade acetonitrile (Fisher Scientific) was used after distillation. Double distilled water was used throughout the study.

Methods. Absorption spectra were recorded on a commercial spectrophotometer (UV-2450, Shimadzu, Japan), and emission spectra were recorded on commercial fluorimeters (FS920CDT, Edinburgh, UK, or FluoroMax-4, Jobin Yvon, USA). ^{1}H NMR spectra were recorded using 500 or 400 MHz NMR spectrometers (Bruker, USA) at 25 °C in deuterated water.

Host−Guest Complex Preparation for NMR Titrations. A guest (5 μL of a 60 mM solution in DMSO-d_6) was added in a step-wise manner to 600 μL of D_2O solution of host OA (from a stock solution of 1 mM OA in 10 mM $Na_2B_4O_7$, pH = 8.7) taken in a NMR tube. After each addition, the solution was shaken, and ^{1}H NMR spectra were recorded. Complex formation was monitored by the upfield shift of the guest

https://dx.doi.org/10.1021/acs.jpca.0c03944
J. Phys. Chem. A 2020, 124, 5297−5305

proton signals. The addition was stopped when there were no changes in the NMR spectra. To check the location MV^{2+} and its influence on the encapsulated guest signals, ^{1}H NMR spectra of solutions containing the 2:1 host/guest complex with incremental amounts of (0.25 equiv) MV^{2+} were recorded. NMR spectra are provided as Figure 2.

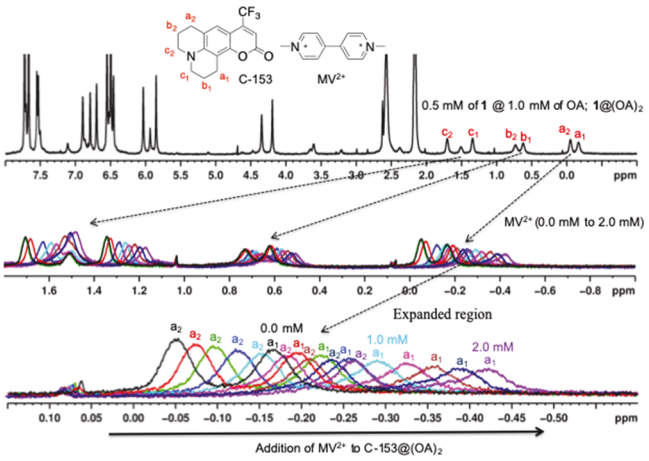

Figure 2. ^{1}H NMR (500 MHz, 10 mM $Na_2B_4O_7$ buffer/D_2O, pH = 8.7) spectra of C153@$(OA)_2$ ([C-153] = 0.5 mM; [OA] = 1 mM) (top), and addition of MV^{2+} to C153@$(OA)_2$ influences the NMR chemical shifts of the guest protons (bottom).

Host–Guest Complex Preparation for Fluorescence Titrations. A stock solution of guest molecule was prepared in dimethyl sulfoxide (DMSO) at 60 mM concentrations. A stock solution of host (OA) solution (12 mL) at 5×10^{-5} M was prepared using 10 mM phosphate buffer/H_2O (pH = 7.4). The solutions of the complexes were prepared by adding 5 μL of a 60 mM guest solution in DMSO (to make final guest concentration 2.5×10^{-5} M) to the as-prepared host solution (5×10^{-5} M). After shaking the mixture manually for 2 min, the solution was placed in a quartz cuvette and bubbled with nitrogen. The emission spectrum of the solution thus prepared was recorded. To this solution, 0.25 equiv increments of MV^{2+} (or BV^{2+}) was added, and emission spectra were recorded upon each addition following bubbling with nitrogen.

Femtosecond Transient Absorption Study. The time-resolved data were acquired on a commercial femtosecond transient absorption spectroscopy setup (FemtoFrame-II, IB Photonics, Bulgaria). The details of the setup are described earlier,[59] and only a brief overview is presented here. The fundamental 800 nm light was obtained from a Ti-sapphire regenerative amplifier (Spitfire Pro XP, Spectra-Physics, USA) pumped by a 20 W Q-switched Nd:YLF laser (Empower, Spectra-Physics, USA) and seeded with a Ti-sapphire femtosecond oscillator (MaiTai SP, Spectra-Physics, USA). The fundamental light thus obtained was divided into two parts. One part was passed through a β-barium borate crystal to generate the 400 nm light, which was used as the pump pulse. The other part of the beam was passed through a delay stage, having a maximum delay time of 2 ns, and focused on a sapphire crystal to generate the white light continuum, which was used as the probe light. After passing through the sample, the probe light was dispersed in a polychromator and detected using a charge-coupled device. For all experiments, the power of the pump light was maintained ~10 μW. The pulse width of the fundamental light was 80 fs, and the instrument response function was measured to be 150 fs.

Cyclic Voltammetry Experiment. Cyclic voltammetry (CV) experiments were performed at room temperature using a commercial electrochemical workstation (600B Series, CH Instruments, USA). A standard three-electrode cell, comprising a glass carbon electrode as the working electrode, platinum wire as the auxiliary electrode, and Ag/AgCl as the reference electrode, was used. No correction was made for liquid junction potential. The CV of donor molecules was measured in acetonitrile solution containing 1.0 mM compound and 0.1 M tetra-*n*-butylammonium hexafluorophosphate as the supporting electrolyte. The CV of viologens was measured using 1.0 mM compound in a 2.0 mM OA solution containing 50 mM NaCl as the supporting electrolyte.

RESULTS

Chemical structures of seven donors and two acceptors used in this study are provided in Figure 1. Complexation of the donors with the host OA was confirmed from their ^{1}H NMR spectra. Several OA–guest complexes probed here have been characterized earlier during our other investigations.[48−51,60] Expected upfield shift of the guest signals was observed upon inclusion within OA. In addition, the diffusion constants measured by DOSY NMR were consistent with that of the capsular assembly.[45,61] ^{1}H NMR titration experiments confirmed the OA–guest complex to be 2:1. In the presence of OA, although the ^{1}H NMR chemical shifts of the donors, as expected, shifted upfield, those of acceptors MV^{2+} and BzV^{2+} were not affected by OA.[48,60] However, diffusion constants of the viologens in the presence of donor@OA_2 were same as that of the complex. These suggested that MV^{2+} and BzV^{2+} were not included within OA but remained attached to the capsule. Interestingly, upon addition of MV^{2+} to C153@OA_2 complex in borate buffer (D_2O), the signals of C153 shifted upfield (Figure 2). This indicated that MV^{2+} influenced the extent of diamagnetic shielding provided by the capsular wall. Obviously, the electronic/magnetic effect of MV^{2+} is able to penetrate the capsular wall and reach the guest molecules present within the capsule. Additional information regarding the interior of the capsule came from the emission maxima of the coumarins[62] and I_1/I_3 value of the Py fluorescence.[63] These suggested that the capsular interior has no water molecules, and the guest alone is present within the OA capsule.[44,45]

Fluorescence of OA-encapsulated guest molecules was quenched by viologen acceptors present in aqueous solution. As representative examples, the spectra for C153@OA_2 in the presence of varying amounts of MV^{2+} and BzV^{2+} are provided in Figure 3. As seen in the figure, upon addition of the viologens, the coumarin emission intensity decreases. Given that the excited singlet-state energies of the viologens are

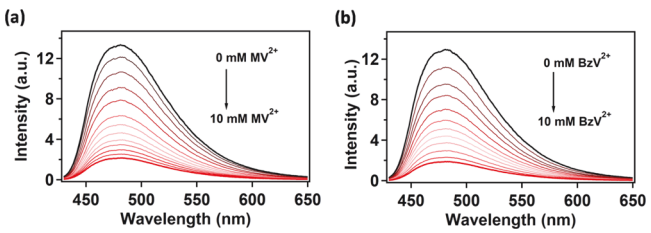

Figure 3. Steady-state emission spectra of C153@OA_2 with gradual addition of (a) MV^{2+} and (b) BzV^{2+} (λ_{exc} = 375 nm).

https://dx.doi.org/10.1021/acs.jpca.0c03944
J. Phys. Chem. A 2020, 124, 5297−5305

higher than that of the entrapped guests, we conclude that the observed decrease is not due to energy transfer, thus confirming that the quenching is because of electron transfer came from identification of the products of electron transfer, the donor cation radical, and the viologen monocation radical. Because of experimental difficulties, the transient absorption spectra of the cation radicals of the coumarins and aromatics, as listed in Figure 1, could not be recorded. However, we have unequivocally identified the formation of stilbene cation radical in the stilbene@OA_2–MV^{2+} system by recording the transient absorption of stilbene cation radical.[60] Based on this observation, we conclude that electron transfer is the primary cause of fluorescence quenching in the donor–acceptor systems investigated here. The transient absorption spectra of monocation radicals of methyl viologen and benzyl viologen (i.e., $MV^{+\bullet}$ and $BzV^{+\bullet}$), the products of electron transfer from the encapsulated excited donors to MV^{2+} and BzV^{2+}, recorded in this study supported this conclusion. Representative transient spectra recorded in the case of C153@OA_2–MV^{2+} are provided in Figure 4. Thus, upon excitation, the donor present within the "dry" OA capsule transfers an electron to the acceptor attached to the exterior wall.

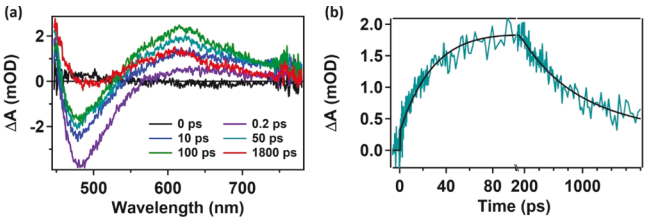

Figure 4. Plot of (a) transient absorption spectra at different time delays (in the early time, stimulated emission of the C153 can be seen and with time, it decreases, and the absorption band at 610 nm, which is because of the formation of $MV^{+\bullet}$, starts to increase) and (b) kinetic trace at 610 nm along with the fit (black solid line) for C153@OA_2 in the presence of 10 mM MV^{2+} (pump pulse: 400 nm, probe: 450–760 nm).

The rates of PET were estimated by monitoring the rise and decay of $MV^{+\bullet}$ and $BzV^{+\bullet}$ by recording their transient spectra following excitation of the encapsulated donors. For these experiments, phosphate buffer (pH ~ 7.4) solutions of 100 μM 1:2 donor@OA_2 complexes and 10 mM viologen (MV^{2+} and BzV^{2+}) were used. To initiate the PET reaction, the encapsulated guest was excited with a 400 nm pump pulse. To ensure the detection of the viologen radical cation that absorbs around 610 nm, transient absorption spectra were recorded from 450–760 nm. In Figure 4, the transient absorption spectra for C153@OA_2 in the presence of MV^{2+} recorded at different time delays following pumping are displayed. The data for remaining systems are provided in the Supporting Information (Figure S1). Quenching of C153-stimulated emission in concurrence with the rise of a new absorption band centered at 610 nm because of $MV^{+\bullet}$ is clearly visible. The rate constants of the formation and decay of the $MV^{+\bullet}$ were extracted from the plot of the change in absorbance at 610 nm with respect to the delay time (Figure 4b). After deconvoluting the Gaussian-shaped instrument response function with 150 fs fwhm, the above curve was fitted with the sum of three exponential functions. The same procedure was followed for all donor@OA_2–acceptor systems (Figure S1 in Supporting Information). The fitting parameters are tabulated in Table 1. For all cases, three exponentials were necessary to satisfactorily fit the data. Of the three, one is the rise component and other two are decay components. We assign the rise component as the inverse of the bimolecular PET rate constant (k_{et}).

In order to correlate k_{et} with exergonicity (ΔG°) of electron transfer as per the Rehm–Weller equation (eq 1),[6,64] we needed to know the oxidation potential of the donor (E_{D/D^+}), reduction potential of the acceptor (E_{A^{2+}/A^+}), Coulombic term $\left(\frac{e^2}{\varepsilon_s r_0}\right)$, and the excitation energy ($E_{0,0}$).

$$\Delta G^\circ = E_{D/D^+} - E_{A^{2+}/A^+} - E_{0,0} - \frac{e^2}{\varepsilon_s r_0} \quad (1)$$

It is important to note that oxidation of the donor occurs within the nonpolar OA capsule while the reduction occurs in aqueous phosphate/borate buffer, under two different environments. In addition, it should be noted that the location of reduction is the exterior of OA capsular wall, where the acceptor is Coulombically attached. Also, following reduction, because the charge reduces only by a unit (from 2+ to 1+), $MV^{+\bullet}$ would still be attached to the capsule. Therefore, it is important to measure the reduction potential of acceptors in aqueous buffer in the presence of OA and the oxidation potential of the donors within the OA capsule. Cyclic voltammetry (CV) was used to estimate the oxidation and reduction potentials of the donor and acceptors in the presence

Table 1. Fitting Parameters of the Kinetic Traces at 610 nm and Rehm–Weller Parameters for All the Donor–Acceptor Pairs

pairs	a_1	τ_1 (ps)	a_2	τ_2 (ps)	a_3	τ_3 (ps)	E_{D/D^+} in ACN (eV)	E_{D/D^+} in OA (eV)	E_{A^{2+}/A^+} in OA (eV)	$E_{0,0}$ (eV)	$\left(\frac{e^2}{\varepsilon_s r_0}\right)$ (eV)	ΔG° (eV)	k_{et} (s^{-1}) × 10^{-12}
C153 + MV^{2+}	−0.00179	31.1	0.00145	694	0.00066	3430	0.89	0.505	−0.655	2.78	0.245	−1.375	0.032
C153 + BzV^{2+}	−0.00204	12.2	0.00143	830	0.00054	2878	0.89	0.505	−0.573	2.78	0.245	−1.457	0.082
Py + MV^{2+}	−0.02629	8.6	0.02198	416	0.02402	3580	1.4	1.015	−0.655	3.42	0.245	−1.505	0.116
An + MV^{2+}	−0.01393	5.5	0.01237	447	0.01331	3640	1.185	0.8	−0.655	3.22	0.245	−1.52	0.180
Py + BzV^{2+}	−0.02064	4.4	0.02336	195	0.03944	6500	1.4	1.015	−0.573	3.42	0.245	−1.587	0.227
An + BzV^{2+}	−0.01118	3.4	0.01021	275	0.01899	4720	1.185	0.8	−0.573	3.22	0.245	−1.602	0.294
C466 + BzV^{2+}	−0.04031	2.8	0.00547	285	0.05029	4550	0.92	0.535	−0.573	3.17	0.245	−1.817	0.357
C480 + MV^{2+}	−0.02612	2.5	0.02373	264	0.01071	2070	0.72	0.335	−0.655	3.06	0.245	−1.825	0.400
C480 + BzV^{2+}	−0.01547	2.5	0.01341	270	0.01161	2300	0.72	0.335	−0.573	3.06	0.245	−1.907	0.400
GAz + MV^{2+}	−0.00664	3.5	0.00128	61	0.00193	8550	0.65	0.265	−0.655	3.3	0.245	−2.135	0.285
Az + MV^{2+}	−0.01020	4.0	0.00805	55	0.00273	1150	0.71	0.325	−0.655	3.47	0.245	−2.245	0.250

https://dx.doi.org/10.1021/acs.jpca.0c03944
J. Phys. Chem. A 2020, 124, 5297–5305

of OA. The reduction potential of MV^{2+} in water with respect to Ag/AgCl is found to be 0.685 V. In the OA medium, it decreased to 0.655 V (ref: Ag/AgCl; for cyclic voltammogram (see Figure S2 of the Supporting Information). The same shift in reduction potential was assumed for BzV^{2+} as well.

However, measurement of the oxidation potentials of donors encapsulated within the OA cavity required an indirect approach. Oxidation potentials of all three coumarin derivatives, An, Py, Az, and Gaz, (Figure 1) are greater than 0.8 V,[65] whereas the electrochemical window for water is only up to 0.8 V.[66] This limited the direct measurement of oxidation potential of donor@OA_2 in water. To overcome this problem, we adopted an indirect method. Employing PTZ, whose oxidation potential is less than 0.8 V,[67] as the standard, we corrected the oxidation potential of others. The oxidation potential of PTZ in acetonitrile with respect to Ag/AgCl was measured to be 0.635 V (Figure S2 in Supporting Information). On the other hand, the oxidation potential of PTZ included within the OA capsule was found to be 0.25 V. Comparing the oxidation potential of PTZ in acetonitrile with that in the OA capsule, it is clear that the oxidation potential decreased by 0.385 V. Using this as the correction factor, we converted the oxidation potential in acetonitrile (Ag/AgCl) of donors to that within the OA_2 capsule. The excitation energy ($E_{0,0}$) required in eq 1 was calculated from the 0−0 band of steady-state absorption and emission spectra.

For the calculation of the last term in eq 1, we needed the values of electronic charge (e), permittivity of the solvent (ϵ_s), which is the product of permittivity of vacuum (ϵ_0) and the relative permittivity of the solvent (ϵ_r), and the separation distance (r_0) between the donor and the acceptor. The separation distance r_0 was estimated to be 8.9 Å for C153@OA_2−MV^{2+} by molecular dynamics (MD) simulation (Figure S3 in Supporting Information).[48] The MD simulation suggests that MV^{2+} resides at the bottom of the capsule rather on the side. Given that all the donors are within the OA cavity, and the structures of MV^{2+} and BzV^{2+} are nearly the same, we have used the same value of r_0 for all other pairs. Considering the nature of the OA wall, ϵ_r is taken as relative permittivity of methyl benzoate (6.6).[68] The estimated values of the Coulombic term are tabulated in Table 1.

DISCUSSION

Results accumulated thus far on donor@OA_2−acceptor systems are summarized below: (a) PET across the OA capsular wall does occur with rate constants varying between 3.2×10^{10} and 4×10^{11} s^{-1} (Table 1). (b) Rate of PET shows a Marcus-type correlation with ΔG° (Figure 5). (c) Remarkably, the above plot exhibits Marcus inversion. (d) NMR spectra support the existence of electronic/magnetic interaction between the capsuled donor (C153) and the acceptor (MV^{2+}) present outside the capsule (Figure 2). (e) MD simulation carried out previously with optimized potentials for liquid simulation-all atom (OPLS-AA) force field and GROMACS software package suggested that the MV^{2+} is located closer to the OA capsule containing three different coumarins (C153).[48] The modeled structure shown in the Supporting Information (Figure S3) is consistent with the NMR spectra mentioned above (Figure 2). (f) Quantum chemical calculations employing the time-dependent density functional theory using the polarizable continuum model carried out earlier suggest that the OA capsule acts as a charge acceptor upon excitation of the encapsulated C153.[47]

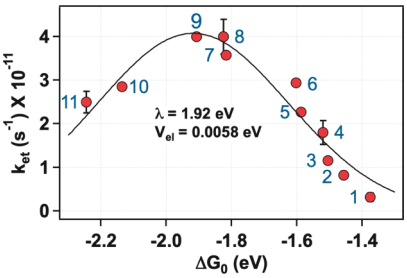

Figure 5. Plot of k_{et} obtained from transient absorption spectroscopy vs the estimated ΔG° for different donor/OA_2−acceptor pairs from 1−11. The pairs from 1−11 are C153@OA_2 + MV^{2+}, C153@OA_2 + BzV^{2+}, Py@OA_2 + MV^{2+}, An@OA_2 + MV^{2+}, Py@OA_2 + BzV^{2+}, An@OA_2 + BzV^{2+}, C466@OA_2 + BzV^{2+}, C480@OA_2 + MV^{2+}, C480@OA_2 + BzV^{2+}, Gaz@OA_2 + MV^{2+}, and Az@OA_2 + MV^{2+}, respectively. The plot was fitted with eq 2. The fitted line is displayed in the black solid line. An experimental error for three representative points is also given.

Apparently, upon excitation, the electron density shifts from C153 to the wall. This unusual behavior is an early indication of what is likely to happen when there is an acceptor adjacent to the wall. (g) Electron-rich character of OA is revealed by fluorescence quenching of excited acceptors such as *N*-methylacridinium iodide, dimethyldiazapyrenium iodide, and dimethyldiazaphenanthrenium iodide by OA.[69] Based on these, the oxidation potential of OA was estimated to be ~1.5 eV. Thus, OA by nature is a good electron donor. (h) With the help of fluorescence probes such as Py, Py aldehyde, and coumarin 1, the interior of the capsule is concluded to be nonpolar and free from water molecules.[45] This suggests that donor molecule's immediate environment would only be the rigid capsular wall. (i) Results of NMR and electron paramagnetic resonance studies revealed that the OA-encapsulated guest molecules have limited freedom of motion within the capsule and they are not frozen as in a glass or solid.[61] (j) Ultrafast solvation dynamic studies have established that the OA capsule-containing guest such as C153 do not disassemble and water do not penetrate into the capsule even in the time scale of 3000 ps following excitation. This implies that the capsule would remain closed during the excited-state lifetimes of the donor.[44] We have found these information to be valuable to interpret the observed correlation between ΔG° and the rates of electron transfer (Figure 5).

The fact that a bell-shaped curve is obtained upon plotting the rate of electron transfer (k_{et}) against ΔG° suggests that the electron transfer across an organic wall investigated here follows the Marcus classical equation. We have calculated the two most important parameters, the reorganization energy (λ) and electronic coupling matrix element (V_{el}) using eq 2

$$k_{et} = \frac{4\pi^2}{h}\frac{{V_{el}}^2}{\sqrt{4\pi\lambda k_B T}} \exp\left\{-\frac{(\Delta G^\circ + \lambda)^2}{4\lambda k_B T}\right\} \quad (2)$$

In the above equation, h is the Planck constant, V_{el} is the electronic coupling matrix element, k_B is the Boltzmann constant, and T is the temperature in K. By fitting the data in Figure 5 into the above equation, we have estimated the λ to be 1.918 eV, and the pre-exponential term to be 4.074×10^{11} s^{-1}. By carrying out the simple arithmetic, the V_{el} was estimated to be 0.0058 eV (see Section S2 of Supporting Information for details).

https://dx.doi.org/10.1021/acs.jpca.0c03944
J. Phys. Chem. A 2020, 124, 5297−5305

We are aware that the λ consists of solvent and nuclear reorganization energies ($\lambda = \lambda_s + \lambda_i$).[6] As discussed above, the encapsulated donor within the OA capsule is surrounded only by the electron-rich rigid capsular organic wall. This rigid wall would not help preparing the excited donor for electron transfer. Thus, λ_s with respect to the donor part is negligible. The acceptor that is already doubly charged (2+) is located adjacent to the capsular exterior wall in water. The acceptor must be surrounded by water molecules and hydrogen bonded to the carboxylate anion of OA. Even after the electron transfer, the solvation is not expected to change significantly around the acceptor because the acceptor would still be positively charged (1+) after accepting an electron from the encapsulated donor molecule and would be attached to the OA wall. Therefore, the solvent reorganization energy term (λ_s) with respect to the acceptor part is also expected to be small. Thus, the λ_s term is negligible during the electron transfer process. Based on these, we believe that the observed λ of 1.918 eV is entirely because of the internal reorganization (λ_i). In rigid media such as glass and melts as well as within the OA capsule, the donor cation radical would be formed in a rigid higher energy environment.[24,70−72] Similarity between our system and these is obvious.

To get an insight into the electron transfer process in a rigid confined environment, we re-examined the Marcus theory of electron transfer. According to this theory, λ is defined as the free energy of the product parabola at the equilibrium nuclear configuration of the reactant parabola, as shown in Figure 6.

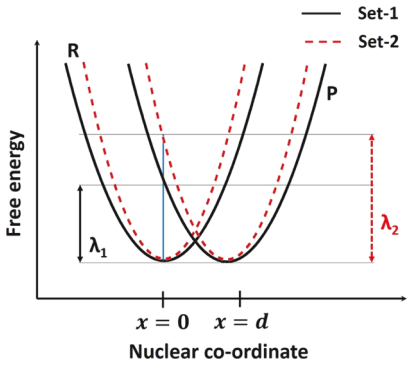

Figure 6. Dependence of reorganization energy on the steepness of the reactant and product parabolas in the Marcus formulation.

Let us consider two sets of reactant and product parabolas. The first set is named set-1 and colored in black, whereas the other one is named set-2 and is colored in red. The only difference between these two sets is that the red parabolas are steeper than the black ones. For both of them, the coordinate of the equilibrium positions of the reactant and product is at $x = 0$ and $x = d$, respectively. Thus, the equations defining the free energy of the reactant ($G_i^R(x)$) and the product ($G_i^P(x)$) parabolas for the i-th set can be written as

$$G_i^R(x) = \frac{1}{2}k_i x^2 \tag{3}$$

$$G_i^P(x) = \frac{1}{2}k_i(x + d)^2 \tag{4}$$

where k_i is the force constant of the parabolas for the i-th set. The solution of the product parabola for $x = 0$ will give the form of λ in terms of k_i and d and is given by

$$\lambda = \frac{1}{2}k_i d^2 \tag{5}$$

Examination of eq 5 reveals that λ increases linearly with increasing k_i. In other words, λ increases as the reactant and product parabolas become steeper. Comparison of the two curves in Figure 6 reveals that when the parabola is steeper (or constricted), more energy will be required to reach the product compared to a wider one, for the same nuclear geometry. In a confined environment like as in the present case, where the structural modification is highly restricted, the reactant and product parabolas are expected to be steeper, leading to a higher value of reorganization energy. In support of our argument, we would like to mention the work on a system of simple harmonic oscillator trapped inside a box and showed that the energy of the oscillator increases with decrease in the box length, leading to a steeper potential.[73]

A similar higher value for λ has been reported in the literature. A high value for λ (2.13 eV) has been noted during reverse electron transfer of radical ion pair by Gould and Farid.[46] In their case, SSRIP possessed higher λ_s (1.63 eV) than the contact radical ion pair (CRIP; 0.48 eV), where the radical cation and radical anion are almost touching each other. In fact, the structure of SSRIP has some similarity to the radical ion pair generated in this supramolecular environment with one exception. In our case, the wall between radical ions is permanent and rigid while in SSRIP, it is flexible and soft.[54] The high λ in this study must all be λ_i while in SSRIP, most of it is likely to be because of λ_s.

The second most important parameter we have retrieved from the Marcus plot is V_{el}. The value of V_{el} depends on the extent of orbital overlap between the donor and the acceptor. For the cases where the orbital overlap for the donor and acceptor is larger, greater will be the value of V_{el}. In our example, like in SSRIP, there is no direct overlap between the donor and the acceptor. A direct comparison between capsular wall-separated radical ion pair with SSRIP is revealing. The V_{el} for CRIP and SSRIP is reported to be 0.093 and 0.00143 eV, respectively.[46] As mentioned earlier, in CRIP, the orbitals of radical ion pair overlap while in SSRIP, there is a solvent molecule in between. The presence of a solvent molecule decreases the orbital overlap and decreases V_{el}. A slightly higher value of V_{el} (0.0058 eV) obtained in our system could be because of the rigidity of the three component systems—donor, capsule, and acceptor. Most likely neither the donor, the acceptor, nor the capsule has much freedom. This is distinctly different from that of SSRIP. We are pleased that our value of V_{el} is closer to that of SSRIP than CRIP.

Another model resembling our system is the C-clamp-trapped solvent-mediated electron transfer.[25−28] One must recognize that unlike the solvent molecule trapped in the C-clamp, the capsular wall that serves as the mediator between a donor and an acceptor has no flexibility or freedom. The electronic coupling between the donor and the acceptor in the C-clamp system is shown to depend on the electronic and steric properties of the solvent. The value of V_{el} varies between 0.0035 and 0.0068 ± 0.00161 eV.[27] Our value is on the higher side and this could be attributed to the dynamic nature of the C-clamp−solvent versus the static nature of the donor@OA_2−acceptor system. Other examples that has some resemblance to ours are the systems in which electron transfer occurs under solvent-free and diffusion-less conditions.[29,31] Under these conditions, the donor and acceptor molecules are preposi-

https://dx.doi.org/10.1021/acs.jpca.0c03944
J. Phys. Chem. A 2020, 124, 5297−5305

tioned adjacent to each other. The examples include dyes adsorbed on single crystals of aromatic molecules and melts of dyes with aromatic molecules. The V_{el} values varied between 0.0023 and 0.0043 eV. The electronic coupling reported for these systems is slightly smaller than what we have calculated for OA wall-mediated electron transfer.

The system that is directly relevant to the current study is the Cram hemicarcerand system investigated by Piotrowiak[36] and Balzani.[39] Electron and energy transfers across this hemicarcerand's wall have been investigated. However, it is important to note that the electron exchange matrix elements calculated for energy transfer between incarcerated triplet biacetyl and aromatic and olefinic acceptors vary between 0.00001 and 0.00003 ± 10% eV and are much smaller than what we have noted in the current system.[37,39] The difference most likely is due to the fact that the acceptors in our system are Coulombically bound to the exterior of the capsule while in the Cram hemicarcerand system, the acceptors are free in solution. Because of the lack of any specific attraction between the hemicarcerand and the acceptor molecules, the contact time between the acceptor and the carcerand will be short while in our case, it is quite long. Interestingly, the electronic coupling is shown to depend on the internal cavity dimension of the Cram-type hemicarcerands.[38] The smaller the capsule, the stronger the coupling. Clearly close interaction between the guest biacetyl and the walls of the hemicarcerand favors stronger coupling.

Expectedly, the V_{el} noted here is smaller than for systems, wherein the donor and acceptor are covalently linked. The observed smaller value is consistent with the expectation that lack of direct σ/π link would decrease the electronic coupling. An interesting but not so obvious feature one should note is that the wall of OA is rich in electron. This is likely to increase the barrier for the electronic coupling between the donor and the acceptor through the wall and reduce the electronic coupling. This is in accordance with what has been noted in the C-clamp−solvent systems.[27] A correlation between electronic coupling and the electron affinity of the solvent has been noted in C-clamp systems.[27] Interestingly, solvent molecules with low electron affinity have smaller electronic coupling. We believe that a similar effect may reduce the coupling between the excited donor and electron-rich capsular wall. However, the calculated V_{el} in this study is higher than that in SSRIP and seems sufficient to bring about electron transport across the capsular wall.

CONCLUSIONS

Overall, one could visualize the OA-encapsulated donor and Coulombically linked acceptor system to be capable of undergoing PET. The capsular wall participates in the electron transfer process. Because the interior of the capsule is dry and rigid, medium reorganization is not expected to provide the needed driving force.[54] The observed λ value is higher than expected while V_{el} is reasonable for the current system. The preliminary quantum chemical calculation suggested that upon excitation of encapsulated coumarin, the charge shifts toward the wall. It seems that when there is an acceptor adjacent to the wall, the charge from the wall moves to the acceptor. Although the model we propose is qualitatively consistent with the observed results, a better understanding is needed, and we are currently pursuing theoretical understanding of the observed phenomenon through collaboration.

ASSOCIATED CONTENT

Supporting Information

The Supporting Information is available free of charge at https://pubs.acs.org/doi/10.1021/acs.jpca.0c03944.

Kinetic traces for the formation of viologen radical cation for different donor@OA_2−viologen pairs, CV data for MV^{2+} and PTZ in bulk solvent and in OA, MD simulation carried out with OPLS-AA force field and GROMACS software package, derivation of the Marcus bell-shaped dependence, calculation of V_{el} from the pre-exponential term, and derivation of the fwhm of Marcus plot (PDF)

AUTHOR INFORMATION

Corresponding Authors

Pratik Sen − *Department of Chemistry, Indian Institute of Technology Kanpur, Kanpur 208 016, Uttar Pradesh, India;* orcid.org/0000-0002-8202-1854; Email: psen@iitk.ac.in

V. Ramamurthy − *Department of Chemistry, University of Miami, Coral Gables, Florida 33146, United States;* orcid.org/0000-0002-3168-2185; Email: murthy1@miami.edu

Authors

Aritra Das − *Department of Chemistry, Indian Institute of Technology Kanpur, Kanpur 208 016, Uttar Pradesh, India*

Nareshbabu Kamatham − *Department of Chemistry, University of Miami, Coral Gables, Florida 33146, United States*

A. Mohan Raj − *Department of Chemistry, University of Miami, Coral Gables, Florida 33146, United States*

Complete contact information is available at: https://pubs.acs.org/10.1021/acs.jpca.0c03944

Notes

The authors declare no competing financial interest.

ACKNOWLEDGMENTS

V.R. thanks the National Science Foundation (CHE-1807729) for financial support. P.S. thanks IIT Kanpur for infrastructure and support. We thank Prof. R. N. Mukherjee of Department of Chemistry, IIT Kanpur for cyclic voltammetry measurements. A.D. thanks Visvesvaraya PhD Program of Ministry of Electronics & Information Technology (MeitY), Government of India for providing graduate fellowship.

REFERENCES

(1) Barbara, P. F.; Meyer, T. J.; Ratner, M. A. Contemporary Issues in Electron Transfer Research. *J. Phys. Chem.* **1996**, *100*, 13148−13168.

(2) Balzani, V. *Electron Transfer in Chemistry*; Wiley: New York, 2001; Vol. *1*−*5*.

(3) Piotrowiak, P. *Solar Energy Conversion: Dynamics of Interfacial Electron and Excitation Transfer*; Royel Society of Chemistry: Cambridge, U.K., 2013.

(4) Fox, M. A.; Chanon, M. *Photoinduced Electron Transfer*; Elseveir: Amsterdam, 1988; Vol. *1*−*4*.

(5) Kavarnos, G. J.; Turro, N. J. Photosensitization by Reversible Electron Transfer: Theories, Experimental Evidence and Examples. *Chem. Rev.* **1986**, *86*, 401−449.

(6) Turro, N. J.; Ramamurthy, V.; Scaiano, J. C. *Modern Molecular Photochemistry of Organic Molecules*; University Science Books: Sausalito, CA, 2010.

(7) Gray, H. B.; Winkler, J. R. Electron Tunneling through Proteins. *Q. Rev. Biophys.* **2003**, *36*, 341−372.
(8) Gray, H. B.; Winkler, J. R. Long-Range Electron Transfer. *Proc. Natl. Acad. Sci.* **2005**, *102*, 3534−3539.
(9) Winkler, J. R.; Gray, H. B. Electron Flow through Metalloproteins. *Chem. Rev.* **2014**, *114*, 3369−3380.
(10) McLendon, G. Long-Distance Electron Transfer in Proteins and Model Systems. *Acc. Chem. Res.* **1988**, *21*, 160−167.
(11) McLendon, G.; Hake, R. Interprotein Electron Transfer. *Chem. Rev.* **1992**, *92*, 481−490.
(12) Davidson, V. L. What Controls the Rates of Interprotein Electron-Transfer Reactions. *Acc. Chem. Res.* **2000**, *33*, 87−93.
(13) Giese, B. Long-Distance Electron Transfer through DNA. *Annu. Rev. Biochem.* **2002**, *71*, 51−70.
(14) Joy, A.; Schuster, G. B. Long-Range Radical Cation Migration in DNA: Investigation of the Mechanism. *Chem. Commun.* **2005**, 2778−2784.
(15) Grinstaff, M. W. How Do Charges Travel through DNA?—an Update on a Current Debate. *Angew. Chem., Int. Ed.* **1999**, *38*, 3629−3635.
(16) Lewis, F. D.; Young, R. M.; Wasielewski, M. R. Tracking Photoinduced Charge Separation in DNA: From Start to Finish. *Acc. Chem. Res.* **2018**, *51*, 1746−1754.
(17) Paddon-Row, M. N. Superexchange-Mediated Charge Separation and Charge Recombination in Covalently Linked Donor-Bridge Acceptor Systems. *Aust. J. Chem.* **2003**, *56*, 729−748.
(18) Closs, G. L.; Miller, J. R. Intramolecular Long-Distance Electron Transfer in Organic Molecules. *Science* **1988**, *240*, 440−447.
(19) Wasielewski, M. R. Photoinduced Electron Transfer in Supramolecular Systems for Artificial Photosynthesis. *Chem. Rev.* **1992**, *92*, 435−461.
(20) Paddon-Row, M. N. Covalently Linked Systems Based on Organic Components. In *Electron Transfer in Chemistry*; Balzani, V., Ed.; Wiley: Weinheim, 2001; Vol. *3*, pp 178−271.
(21) Miller, J. R.; Beitz, J. V. Long Range Transfer of Positive Charge between Dopant Molecules in a Rigid Glassy Matrix. *J. Chem. Phys.* **1981**, *74*, 6746−6756.
(22) Miller, J. R.; Beitz, J. V.; Huddleston, R. K. Effect of Free Energy on Rates of Electron Transfer between Molecules. *J. Am. Chem. Soc.* **1984**, *106*, 5057−5068.
(23) Wenger, O. S.; Leigh, B. S.; Villahermosa, R. M.; Gray, H. B.; Winkler, J. R. Electron Tunneling through Organic Molecules in Frozen Glasses. *Science* **2005**, *307*, 99−102.
(24) Chen, P.; Meyer, T. J. Electron Transfer in Frozen Media. *Inorg. Chem.* **1996**, *35*, 5520−5524.
(25) Han, H.; Zimmt, M. B. Solvent-Mediated Electron Transfer: Correlation between Coupling Magnitude and Solvent Vertical Electron Affinity. *J. Am. Chem. Soc.* **1998**, *120*, 8001−8002.
(26) Kaplan, R. W.; Napper, A. M.; Waldeck, D. H.; Zimmt, M. B. Solvent Mediated Coupling across 1 Nm: Not a Π Bond in Sight. *J. Am. Chem. Soc.* **2000**, *122*, 12039−12040.
(27) Napper, A. M.; Read, I.; Kaplan, R.; Zimmt, M. B.; Waldeck, D. H. Solvent Mediated Superexchange in a C-Clamp Shaped Donor-Bridge-Acceptor Molecule: The Correlation between Solvent Electron Affinity and Electronic Coupling. *J. Phys. Chem. A* **2002**, *106*, 5288−5296.
(28) Read, I.; Napper, A.; Kaplan, R.; Zimmt, M. B.; Waldeck, D. H. Solvent-Mediated Electronic Coupling: The Role of Solvent Placement. *J. Am. Chem. Soc.* **1999**, *121*, 10976−10986.
(29) Kemnitz, K. Diffusionless Homogeneous Electron Transfer. Determination of the through-Space Electron-Exchange Matrix Element of Aromatic Donor-Acceptor Pairs. *Chem. Phys. Lett.* **1988**, *152*, 305−310.
(30) Kemnitz, K.; Yoshihara, K. Diffusionless Electron Transfer of Xanthene Dyes in Nonpolar and Weakly Polar Donar-and Acceptor-Solvents. *Chem. Lett.* **1991**, *20*, 645−648.
(31) Kemnitz, K.; Nakashima, N.; Yoshihara, K. Electron Transfer by Isolated Rhodamine B Molecules Adsorbed on Organic Single Crystals. A Solvent-Free Model System. *J. Phys. Chem.* **1988**, *92*, 3915−3925.
(32) Cram, D. J.; Cram, J. M. *Container Molecules and Their Guests*; Royal Society of Chemistry: Cambridge, 1997.
(33) Jankowska, K. I.; Pagba, C. V.; Chekler, E. L. P.; Deshayes, K.; Piotrowiak, P. Electrostatic Docking of a Supramolecular Host-Guest Assembly to Cytochrome C Probed by a Bidirectional Photoinduced Electron Transfer. *J. Am. Chem. Soc.* **2010**, *132*, 16423−16431.
(34) Pagba, C.; Zordan, G.; Galoppini, E.; Piatnitski, E. L.; Hore, S.; Deshayes, K.; Piotrowiak, P. Hybrid Photoactive Assemblies: Electron Injection from Host-Guest Complexes into Semiconductor Nanoparticles. *J. Am. Chem. Soc.* **2004**, *126*, 9888−9889.
(35) Piotrowiak, P. Photoinduced Electron Transfer in Molecular Systems: Recent Developments. *Chem. Soc. Rev.* **1999**, *28*, 143−150.
(36) Piotrowiak, P.; Deshayes, K.; Romanova, Z. S.; Pagba, C.; Hore, S.; Zordan, G.; Place, I.; Farrán, A. Electron and Excitation Transfer in Hetero-Supramolecular Assemblies and at Molecule-Nanoparticle Interfaces. *Pure Appl. Chem.* **2003**, *75*, 1061−1068.
(37) Place, I.; Farran, A.; Deshayes, K.; Piotrowiak, P. Triplet Energy Transfer through the Walls of Hemicarcerands: Temperature Dependence and the Role of Intrernal Reorganization Energy. *J. Am. Chem. Soc.* **1998**, *120*, 12626−12633.
(38) Romanova, Z. S.; Deshayes, K.; Piotrowiak, P. Triplet Excitation Transfer through the Walls of Hemicarcerands: Dependence of the Electronic Coupling on the Size of the Molecular Cage. *J. Am. Chem. Soc.* **2001**, *123*, 11029−11036.
(39) Parola, A. J.; Pina, F.; Ferreira, E.; Maestri, M.; Balzani, V. Photoinduced Electron- and Energy-Transfer Processes of Biacetyl Imprisoned in a Hemicarcerand. *J. Am. Chem. Soc.* **1996**, *118*, 11610−11616.
(40) Gibb, C. L. D.; Gibb, B. C. Well-Defined, Organic Nanoenvironments in Water: The Hydrophobic Effect Drives a Capsular Assembly. *J. Am. Chem. Soc.* **2004**, *126*, 11408−11409.
(41) Jayaraj, N.; Zhao, Y.; Parthasarathy, A.; Porel, M.; Liu, R. S. H.; Ramamurthy, V. Nature of Supramolecular Complexes Controlled by the Structure of the Guest Molecules: Formation of Octa Acid Based Capsuleplex and Cavitandplex. *Langmuir* **2009**, *25*, 10575−10586.
(42) Thomas, S. S.; Tang, H.; Gaudes, A.; Baggesen, S. B.; Gibb, C. L. D.; Gibb, B. C.; Bohne, C. Tuning the Binding Dynamics of a Guest-Octaacid Capsule through Non-Covalent Anchoring. *J. Phys. Chem. Lett.* **2017**, *8*, 2573−2578.
(43) Jayaraj, N.; Jockusch, S.; Kaanumalle, L. S.; Turro, N. J.; Ramamurthy, V. Dynamics of Capsuleplex Formed between Octaacid and Organic Guest Molecules - Photophysical Techniques Reveal the Opening and Closing of Capsuleplex. *Can. J. Chem.* **2011**, *89*, 203−213.
(44) Das, A.; Sharma, G.; Kamatham, N.; Prabhakar, R.; Sen, P.; Ramamurthy, V. Ultrafast Solvation Dynamics Reveal the Octa Acid Capsule's Interior Dryness Depends on the Guest. *J. Phys. Chem. A* **2019**, *123*, 5928−5936.
(45) Porel, M.; Jayaraj, N.; Kaanumalle, L. S.; Maddipatla, M. V. S. N.; Parthasarathy, A.; Ramamurthy, V. Cavitand Octa Acid Forms a Nonpolar Capsuleplex Dependent on the Molecular Size and Hydrophobicity of the Guest. *Langmuir* **2009**, *25*, 3473−3481.
(46) Gould, I. R.; Farid, S. Dynamics of Bimolecular Photoinduced Electron-Transfer Reactions. *Acc. Chem. Res.* **1996**, *29*, 522−528.
(47) Bhandari, S.; Zheng, Z.; Maiti, B.; Chuang, C.-H.; Porel, M.; You, Z.-Q.; Ramamurthy, V.; Burda, C.; Herbert, J. M.; Dunietz, B. D. What Is the Optoelectronic Effect of the Capsule on the Guest Molecule in Aqueous Host/Guest Complexes? A Combined Computational and Spectroscopic Perspective. *J. Phys. Chem. C* **2017**, *121*, 15481−15488.
(48) Chuang, C.-H.; Porel, M.; Choudhury, R.; Burda, C.; Ramamurthy, V. Ultrafast Electron Transfer across a Nanocapsular Wall: Coumarins as Donors, Viologen as Acceptor, and Octa Acid Capsule as the Mediator. *J. Phys. Chem. B* **2018**, *122*, 328−337.
(49) Raj, A. M.; Porel, M.; Mukherjee, P.; Ma, X.; Choudhury, R.; Galoppini, E.; Sen, P.; Ramamurthy, V. Ultrafast Electron Transfer from Upper Excited State of Encapsulated Azulenes to Acceptors

https://dx.doi.org/10.1021/acs.jpca.0c03944
J. Phys. Chem. A 2020, 124, 5297−5305

across an Organic Molecular Wall. *J. Phys. Chem. C* **2017**, *121*, 20205−20216.
(50) Porel, M.; Chuang, C.-H.; Burda, C.; Ramamurthy, V. Ultrafast Photoinduced Electron Transfer between an Incarcerated Donor and a Free Acceptor in Aqueous Solution. *J. Am. Chem. Soc.* **2012**, *134*, 14718−14721.
(51) Porel, M.; Klimczak, A.; Freitag, M.; Galoppini, E.; Ramamurthy, V. Photoinduced Electron Transfer across a Molecular Wall: Coumarin Dyes as Donors and Methyl Viologen and Tio2 as Acceptors. *Langmuir* **2012**, *28*, 3355−3359.
(52) Ramamurthy, V.; Jockusch, S.; Porel, M. Supramolecular Photochemistry in Solution and on Surfaces: Encapsulation and Dynamics of Guest Molecules and Communication between Encapsulated and Free Molecules. *Langmuir* **2015**, *31*, 5554−5570.
(53) Ponce, A.; Gray, H. B.; Winkler, J. R. Electron Tunneling through Water: Oxidative Quenching of Electronically Excited $Ru(Tpy)_2^{2+}$ (Tyy = 2,2':6,2"-Terpyridine) by Ferric Ions in Aqueous Glasses at 77 K. *J. Am. Chem. Soc.* **2000**, *122*, 8187−8191.
(54) Ramamurthy, V.; Weiss, R. G.; Hammond, G. S. *A Model for the Influence of Organized Media on Photochemical Reactions*; John Wiley & Sons, Inc.: New York, 1993; Vol. *18*, pp 67−234.
(55) Marcus, R. A.; Sutin, N. Electron Transfers in Chemistry and Biology. *Biochim. Biophys. Acta, Rev. Bioenerg.* **1985**, *811*, 265−322.
(56) Marcus, R. A. Tutorial on Rate Constants and Reorganization Energies. *J. Electroanal. Chem.* **2000**, *483*, 2−6.
(57) Marcus, R. A. Electron Transfer Reactions in Chemistry: Theory and Experiement (Nobel Lecture). *Angew. Chem., Int. Ed.* **1993**, *32*, 1111−1222.
(58) Marcus, R. A. Chemical and Electrochemical Electron-Transfer Theory. *Annu. Rev. Phys. Chem.* **1964**, *15*, 155−196.
(59) Mukherjee, P.; Das, A.; Sengupta, A.; Sen, P. Bimolecular Photoinduced Electron Transfer in Static Quenching Regime: Illustration of Marcus Inversion in Micelle. *J. Phys. Chem. B* **2017**, *121*, 1610−1622.
(60) Porel, M.; Jockusch, S.; Parthasarathy, A.; Rao, V. J.; Turro, N. J.; Ramamurthy, V. Photoinduced Electron Transfer between a Donar and an Acceptor Separated by a Capsular Wall. *Chem. Commun.* **2012**, *48*, 2710−2712.
(61) Kulasekharan, R.; Jayaraj, N.; Porel, M.; Choudhury, R.; Sundaresan, A. K.; Parthasarathy, A.; Ottaviani, M. F.; Jockusch, S.; Turro, N. J.; Ramamurthy, V. Guest Rotations within a Capsuleplex Probed by NMR and EPR Techniques. *Langmuir* **2010**, *26*, 6943−6953.
(62) Jones, G.; Jackson, W. R.; Choi, C. Y.; Bergmark, W. R. Solvent Effects on Emission Yield and Lifetime for Coumarin Laser Dyes. Requirements for a Rotatory Decay Mechanism. *J. Phys. Chem. C* **1985**, *89*, 294−300.
(63) Kalyanasundaram, K.; Thomas, J. K. Enviromental Effects on Vibronic Band Intensities in Pyrene Monomer Fluorescence and Their Application in Studies of Micellar Systems. *J. Am. Chem. Soc.* **1977**, *99*, 2039−2044.
(64) Rehm, D.; Weller, A. Kinetics of Fluorescence Quenching by Electron and H-Atom Transfer. *Isr. J. Chem.* **1970**, *8*, 259−271.
(65) Pysh, E. S.; Yang, N. C. Polarographic Oxidation Potentials of Aromatic Compounds. *J. Am. Chem. Soc.* **1963**, *85*, 2124−2130.
(66) Zoski, C. G. *Handbook of Electrochemistry*; Elsevier: Amsterdam, 2006.
(67) Paduszek, B.; Kalinowski, M. K. Redox Behaviour of Phenothiazine and Phenazine in Organic Solvents. *Electrochim. Acta* **1983**, *28*, 639−642.
(68) Murakami, R.; Kobayashi, S.; Okazaki, M.; Bismarck, A.; Yamamoto, M. Effects of Contact Angle and Flocculation of Particles of Oligomer of Tetrafluoroethylene on Oil Foaming. *Front. Chem.* **2018**, *6*, 435.
(69) Jagadesan, P.; Mondal, B.; Parthasarathy, A.; Rao, V. J.; Ramamurthy, V. Photochemical Reaction Containers as Energy and Electron-Transfer Agents. *Org. Lett.* **2013**, *15*, 1326−1329.
(70) Harriman, A.; Heitz, V.; Ebersole, M.; van Willigen, H. Intramolecular Electron and Energy Transfer within a Bisporphyrin in a Low-Temperature Glass. *J. Phys. Chem.* **1994**, *98*, 4982−4989.
(71) Gaines, G. L.; O'Neil, M. P.; Svec, W. A.; Niemczyk, M. P.; Wasielewski, M. R. Photoinduced Electron Transfer in the Solid State: Rate Vs. Free Energy Dependence in Fixed-Distance Porphyrin-Acceptor Molecules. *J. Am. Chem. Soc.* **1991**, *113*, 719−721.
(72) Wasielewski, M. R.; Johnson, D. G.; Svec, W. A.; Kersey, K. M.; Minsek, D. W. Achieving High Quantum Yield Charge Separation in Porphyrin-Containing Donor-Acceptor Molecules at 10 K. *J. Am. Chem. Soc.* **1988**, *110*, 7219−7221.
(73) Consortini, A.; Frieden, B. R. Quantum-Mechanical Solution for the Simple Harmonic Oscillator in a Box. *Il Nuovo Cimento B* **1976**, *35*, 153−164.

https://dx.doi.org/10.1021/acs.jpca.0c03944
J. Phys. Chem. A 2020, 124, 5297−5305